Geophys. J. Int. (2004) **157,** 753–763 doi: 10.1111/j.1365-246X.2004.02242.x

Anisotropic migration weight for amplitude-preserving migration and sensitivity analysis

D. Kiyashchenko,[1] B. Kashtan[1] and R.-E. Plessix[2]

[1]*State University of Saint-Petersburg,* 1 *Ulianovskaya Street, St Petersburg* 199504, *Russia*
[2]*Shell International E&P,* PO Box 60, 2280 *AB Rijswijk, the Netherlands. E-mail: ReneEdouard.Plessix@shell.com*

Accepted 2004 January 4. Received 2003 October 24; in original form 2003 May 6

SUMMARY

An amplitude-preserving anisotropic migration formula is derived in this paper. The migration is viewed as a weighted diffraction stack and the migration weights are estimated with the stationary phase theorem. To obtain a formula easy to implement, the weights are written in terms of quantities computable along the rays. A sensitivity analysis is then carried out to show that, in the vertical transverse isotropic case, the amplitude-preserving migration is mainly governed by two parameters: the anisotropic NMO velocity and the parameter η. These parameters can be estimated from the data with a velocity (background) analysis. Therefore, it is possible to use this amplitude-preserving anisotropic migration to recover the correct amplitudes versus offset or azimuth in the migrated image.

Key words: anisotropy, migration weights, ray tracing.

1 INTRODUCTION

Amplitude-preserving depth migration is a crucial tool to perform amplitude versus angle (or versus azimuth) (AVO/AVA) analysis over complex geological structures. Different formulations of this problem have been studied over the last 20 years. It has been recognized that the anisotropic nature of the earth can play an important role and needs to be incorporated in migration algorithms. It is relatively easy to implement an algorithm for pre-stack depth migration in an anisotropic medium, with a purpose of inner interface recovery only. However, in order to design amplitude preserving algorithms taking into account the anisotropy of the medium, the corresponding migration weights should be derived.

Based on the high-frequency approximation, which corresponds to the zero-order ray theory, two approaches have been used to derive amplitude-preserving migration weights. One approach formulates the migration as an inverse problem. The migration can then be viewed as the inverse of the forward operator. Under the high-frequency approximation, the scattered field is expressed as an integral operator and the migration corresponds to a general Radon transform (Beylkin 1985). This approach leads to the famous amplitude-preserving migration algorithm based on Beylkin's determinant. The original work has been extended over the years to elastic and multi-valued cases (Miller *et al.* 1987; Beylkin & Burridge 1990; ten Kroode *et al.* 1994). In the 1980s, it was also recognized that the migration is similar to the gradient with respect to the velocity model of the least-squares functional between the observed data and the synthetic data (Lailly 1983; Tarantola 1984). This formulation leads to the iterative migration. Using the Born approximation, for the isotropic acoustic and elastic cases, amplitude-preserving migrations have been derived by approximating the Hessian of the least-squares functional (Chavent & Plessix 1999; Jin *et al.* 1992; Lambaré *et al.* 1992, 2003; Thierry *et al.* 1999).

The other approach is based on the Kirchhoff integral (the diffraction stack method) and the imaging principle. This leads to a Kirchhoff migration/inversion formula (Bleistein 1987; Docherty 1991). Notice that the two approaches are strongly related in practice (Jin *et al.* 1992). In the Kirchhoff approach, the result of a weighted diffraction stack is viewed as an angle-dependent reflectivity. Different methods have been proposed to evaluate the weights (Bortfeld 1989; Docherty 1991; Keho & Beydoun 1988; Schleicher *et al.* 1993). Although some of the notations may differ, they lead to similar migration weights (Hanitzsch 1997). In this paper, the Kirchhoff heuristic approach is followed to estimate the migration weights for the anisotropic case. The displacement at the earth surface is expressed with zero-order approximation of the ray theory (Babič 1994). After Fourier transform, the weighted diffraction stack can be evaluated with the stationary phase theorem. Then the migration weights are expressed with quantities computable along the rays from the source or the receiver to the scattered points to provide a formula easy to implement.

The anisotropic weights described in this paper are valid for any kind of anisotropy. However, just a small set of parameters of the background media can actually be known. Under the assumption of vertical transverse isotropy, a sensitivity analysis is carried out in order to determine an optimal set of parameters governing the amplitude-preserving anisotropic migration. The sensitivity to Thomsen's parameters (Thomsen 1986), ε and δ, and the parameters η and V_{NMO} (Alkalifah 1997) show the importance of the two last parameters for small-to-medium incidence angles, which corroborates the results of (Alkalifah 1997; Alkalifah & Rampton 2001; Plessix & Bork 1998). This parametrization may differ from the one needed for the AVO/AVA inversion (Plessix & Bork 2000). Indeed, on one hand, the migration is governed by the propagation of the waves and, therefore, by the average values (integral values over the ray path) of the model parameters. On the other hand the AVO/AVA analysis depends on the local values of the parameters around the interface.

In this paper, the anisotropic amplitude preserving migration weights are derived following Babič's notation and using the basis of paraxial ray theory. This approach, which neglects the presence of caustics, has been described in Schleicher *et al.* (1993) for the elastic case. The formula corresponds to a shot-based migration. In the Appendices, the formulae are rewritten using Červený's notations. Results on simple layered examples are then shown. Finally a sensitivity analysis is performed.

2 SHOT-BASED AMPLITUDE PRESERVING MIGRATION

2.1 Forward model

To derive the migration weights, a forward model based on a simple model is considered. The model consists of two half spaces separated by an interface represented by $F(\mathbf{x}) = 0$ in the Cartesian coordinate system $\mathbf{x} = (x_1, x_2, x_3)$. The function F is assumed differentiable in order to define the normal to the interface. For the forward model, the earth parameters above and below the interface are known, therefore the classic continuity conditions at the interface give the reflectivity, i.e. the reflection coefficients, κ. For the migration, only the earth parameters above the interface will be assumed, the interface is not known. The goal will be to recover the reflectivity and the location of the interface. To simplify the notation, the source is at the origin, point (0, 0, 0), and the receivers are in the plane $x_3 = 0$.

With the zero-order approximation of the ray theory for inhomogeneous anisotropic medium, the reflected wavefield can be expressed as (Babič 1994):

$$\mathbf{u}^{(q)}(\mathbf{x}_r, t) = \kappa^{(q)} \frac{\varphi(\alpha, \beta)}{\sqrt{\rho J(\tau, \alpha, \beta)}} \frac{\sqrt{|(\mathbf{g}^{(+)}, \mathbf{n})|}}{\sqrt{|(\mathbf{g}^{(-)}, \mathbf{n})|}} \mathbf{A}^{(q)} s[t - \tau_r^{(q)}(\mathbf{x}_r)]. \tag{1}$$

with

(i) $\mathbf{u}^{(q)}$: the displacement vector of the reflected q-type wave;
(ii) (τ, α, β): the ray parameters, τ is the traveltime, α the latitudinal angle of the slowness vector and β the longitudinal angle of the slowness vector at the source point;
(iii) $\mathbf{x}_r$: the observation point;
(iv) $\kappa^{(q)}$: the reflection coefficient at the reflection point;
(v) ρ: the density of the medium at the observation point;
(vi) $\mathbf{n}$: the normal to the interface $F(\mathbf{x}) = 0$ at the reflection point;
(vii) $\mathbf{g}^{(-)}, \mathbf{g}^{(+)}$: the ray velocities of incident and reflected wave at the reflection point;
(viii) $\mathbf{A}^{(q)}$: the unit polarization vector of the q-type reflected wave at the observation point;
(ix) $\varphi(\alpha, \beta)$: the pattern diagram of the source;
(x) $\tau_r^{(q)}(\mathbf{x}_r)$: the traveltime of the q-type reflected wave from the source (0, 0, 0) to the point of observation via the reflection point;
(xi) $\mathbf{x} = (x_1, x_2, x_3)$;
(xii) $s(t)$: the wavelet of the source;
(xiii) $J(\tau, \alpha, \beta)$: the Jacobian of the transformation from the general cartesian coordinate system (x_1, x_2, x_3) to the ray coordinate system (τ, α, β), calculated at the observation point.

The reflections on the free surface are not considered in eq. (1), but the free surface condition can be taken into account by modifying the source wavelet and the pattern diagram as it is done with the isotropic formulae. Eq. (1) models one branch in case of multivalueness.

In the following, only the projection of the displacement vector, $\mathbf{u}^{(q)}$, onto a direction described by the unit vector $\mathbf{d}$ will be considered. The scalar field, u, is:

$$u(\mathbf{x}_r, t) \equiv [\mathbf{u}^{(q)}(\mathbf{x}_r, t), \mathbf{d}]. \tag{2}$$

In the examples, the direction of the projection is the axis x_3, namely $\mathbf{d} = (0, 0, 1)^T$. This corresponds to the vertical component. To simplify the notation, the index (q) is omitted.

2.2 Migration formula

Following the heuristic idea of Kirchhoff migration that the migration can be viewed as a weighted diffraction stack (Docherty 1991; Hanitzsch 1997) and assuming, for the moment, that the weights are constant and equal to 1, the image at the scattered point $\mathbf{x} = (x_1, x_2, x_3)$ is expressed in three dimensions by the double integral:

$$m(\mathbf{x}) = \int_{-\infty}^{\infty} \int_{-\infty}^{\infty} u[\mathbf{x}_r, \tau_d(\mathbf{x}_r, \mathbf{x})] \, d\mathbf{x}_r; \tag{3}$$

where the diffracted traveltime, $\tau_d(\mathbf{x}_r, \mathbf{x})$, is the sum of the propagation time from the source (0, 0, 0) to the image (scattered) point, I, and the propagation time from the image (scattered) point, I, to the receiver $\mathbf{x}_r = (x_1, x_2, x_3 = 0)$ (see Fig. 1). Here the diffraction and reflection terms have the meaning explained in (Schleicher *et al.* 1993). The diffraction traveltime corresponds to the ray connecting the source and the receiver through the scattered point, I, this is the computed traveltime. The reflection traveltime corresponds to the ray connecting the source and the receiver through the reflection point, R, this is the real (observed) time.

Notice that the interface F and the reflection point R, in Fig. 1, are not known during the migration. It is possible to prove with the stationary phase theorem and the high-frequency approximation that if the source wavelet is equal to $\delta'(t)$ the function $m(\mathbf{x})$, eq. (3), is

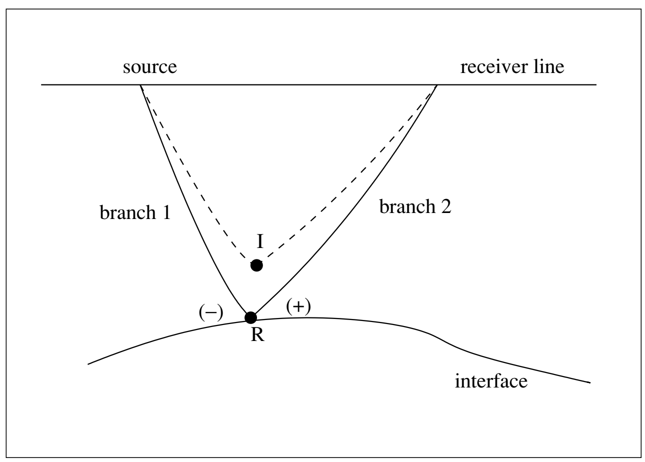

Figure 1. The model: I is an image (scattered)point, used during the migration; R is the reflection point on the interface (I and R coincide when the model is correct); dash line: 'diffracted' ray; solid line: reflected ray. Branch 1 connects the source to the reflection or scattered point, branch 2 connects the reflection or scattered point to the receiver.

equal to

$$m(\mathbf{x}) \approx \psi(\mathbf{x})\, \delta[F(\mathbf{x})], \tag{4}$$

where δ is the Dirac distribution and ψ an arbitrary smooth function, and as long as an infinite aperture is kept in the integral, eq. (3). Therefore, if the model parameters used to migrate the data are correct, the migrated image has maximal values on the real reflector interface F.

The idea of the amplitude-preserving migration is to include a weight function, $w(\mathbf{x}_r)$, in the diffraction stack, eq. (3), in order to retrieve the reflection coefficients $\kappa(\mathbf{x})$ of the incident wave on the interface. This is similar to the weighted Kirchhoff migration as explained in (Schleicher *et al.* 1993) for instance. The migrated image is then defined by the weighted diffraction stack

$$m_w(\mathbf{x}) = \int_{-\infty}^{\infty}\int_{-\infty}^{\infty} u(\mathbf{x}_r, \tau_d) w(\mathbf{x}_r)\, d\mathbf{x}_r. \tag{5}$$

(Some of the dependencies are not explicitly written.)

This leads to an amplitude-preserving migration if the amplitude of the image is proportional to the reflection coefficient:

$$m_w(\mathbf{x}) \approx \kappa(\mathbf{x})\delta[F(\mathbf{x})]. \tag{6}$$

2.3 Calculation of the weight function

To estimate the weight function, the wavefield, u, eq. (1), is transformed in the Fourier domain, then the expression is plugged into the weighted diffraction stacked, eq. (5), and finally the integral is evaluated with the stationary phase theorem.

In this work, the Fourier transform is, with Re the real part:

$$s(t) = \frac{1}{\pi}\mathrm{Re}\int_0^{\infty} S(\omega) e^{i\omega t}\, d\omega \tag{7}$$

Substituting u by eq. (1) after Fourier transform into eq. (5) gives the weighted migrated image, m_w:

$$m_w(\mathbf{x}) = \frac{1}{\pi}\mathrm{Re}\int_0^{\infty} S(\omega)\, d\omega \int_{-\infty}^{\infty}\int_{-\infty}^{\infty} \kappa \frac{\varphi(\alpha,\beta)}{\sqrt{\rho J(\tau,\alpha,\beta)}}(\mathbf{A},\mathbf{d})$$
$$\frac{\sqrt{|(\mathbf{g}^{(+)},\mathbf{n})|}}{\sqrt{|(\mathbf{g}^{(-)},\mathbf{n})|}} e^{-i\omega[\tau_r(\mathbf{x}_r)-\tau_d(\mathbf{x}_r,\mathbf{x})]} w(\mathbf{x}_r)\, d\mathbf{x}_r. \tag{8}$$

The inner integral can be estimated with the stationary phase theorem. Thereby

$$m_w(\mathbf{x}) \sim \kappa(\hat\alpha,\hat\beta)$$
$$\frac{\varphi(\hat\alpha,\hat\beta) w(\hat{\mathbf{x}}_r)}{\sqrt{\rho(\hat{\mathbf{x}}_r) J(\hat\tau,\hat\alpha,\hat\beta)}}(\mathbf{A}(\hat\tau,\hat\alpha,\hat\beta),\mathbf{d}) \frac{2}{\sqrt{|\det(\Psi)|}} \frac{\sqrt{|(\hat{\mathbf{g}}^{(+)},\mathbf{n})|}}{\sqrt{|(\hat{\mathbf{g}}^{(-)},\mathbf{n})|}}$$
$$\mathrm{Re}\left(e^{-i\frac{\pi}{4}\mathrm{sig}(\Psi)}\int_0^{\infty} S(\omega)\frac{1}{\omega} e^{-i\omega[\tau_r(\hat{\mathbf{x}}_r)-\tau_d(\hat{\mathbf{x}}_r,\mathbf{x})]} d\omega\right), \tag{9}$$

where the symmetric two-by-two matrix Ψ represents the second derivatives of the phase argument with respect to the space coordinates $\mathbf{x}_r = (x_1, x_2, 0)$ taken at the stationary point. For $i, k = 1, 2$

$$\Psi_{ik} = \frac{\partial^2(\tau_r(\mathbf{x}_r) - \tau_d(\mathbf{x}_r,\mathbf{x}))}{\partial x_i \partial x_k}\Big|_{(\mathbf{x}_r=\hat{\mathbf{x}}_r)}. \tag{10}$$

In eq. (9), it is assumed that $\sqrt{|\det(\Psi)|}$ is non zero. This formula is then valid outside the caustic points. sig(Ψ) denotes the signature of the matrix Ψ, which is the number of the positive eigenvalues minus the number of the negative eigenvalues of the matrix. The quantities marked with ˆ are evaluated at the stationary point where the first derivative of the phase argument is equal to zero:

$$\frac{\partial}{\partial x_i}(\tau_r(\hat{\mathbf{x}}_r) - \tau_d(\hat{\mathbf{x}}_r,\mathbf{x})) = 0. \tag{11}$$

Notice that when the image/scattered point coincides with the reflection point, the phase, which corresponds to the difference of the traveltimes, is equal to zero:

$$\tau_r(\hat{\mathbf{x}}_r) - \tau_d(\hat{\mathbf{x}}_r,\mathbf{x}) = 0. \tag{12}$$

Eq. (9) thereby becomes:

$$m_w(\mathbf{x}) \sim \frac{\varphi(\hat\alpha,\hat\beta) w(\hat{\mathbf{x}}_r)}{\sqrt{\rho(\hat{\mathbf{x}}_r) J(\hat\tau,\hat\alpha,\hat\beta)}}(\mathbf{A}(\hat\tau,\hat\alpha,\hat\beta),\mathbf{d}) \frac{2\kappa(\hat\alpha,\hat\beta)}{\sqrt{|\det(\Psi)|}}$$
$$\frac{\sqrt{|(\hat{\mathbf{g}}^{(+)},\mathbf{n})|}}{\sqrt{|(\hat{\mathbf{g}}^{(-)},\mathbf{n})|}}\mathrm{Re}\Big(e^{-i\frac{\pi}{4}\mathrm{sig}(\Psi)}\int_0^{\infty} S(\omega)\frac{1}{\omega} d\omega\Big). \tag{13}$$

An amplitude-preserving migration is obtained when $\mathbf{m}_w$ is proportional to κ, namely when

$$w(\hat{\mathbf{x}}_r) \sim \frac{\sqrt{\rho(\hat{\mathbf{x}}_r) J(\hat\tau,\hat\alpha,\hat\beta)|\det(\Psi)|}}{\varphi(\hat\alpha,\hat\beta)(\mathbf{A}(\hat\tau,\hat\alpha,\hat\beta),\mathbf{d})} \frac{\sqrt{|(\hat{\mathbf{g}}^{(-)},\mathbf{n})|}}{\sqrt{|(\hat{\mathbf{g}}^{(+)},\mathbf{n})|}} \tag{14}$$

This formula is the anisotropic equivalent of the isotropic migration weights described in (Goldin 1989; Schleicher *et al.* 1993), which are closely related to the migration weights obtained with Born approximation and a least-squares formalism (Jin *et al.* 1992). The source term has been omitted in these migration weights, this means that the migrated image corresponds to the reflectivity convolved with the source. In the case of multivalueness the above formulae take into account only one branch. The calculation assumes that the reflection coefficient is real and does not depend on the frequency. This means that the reflection is subcritical and the reflector is represented by a single interface. In principle the complex (overcritical) reflection coefficients can be recovered using the approach described in this paper. In this case it is necessary to migrate the analytical signal instead of real data in eq. (1) and remove the real part in eqs (7), (8), (9) and (13).

2.4 New expression of the weight function

The quantities $J \det(\Psi)$ in eq. (14) are not directly computable with the dynamic ray tracing. In this section a new expression is derived. This is achieved with the help of the transformation matrices **P** and **Q**. These matrices can be computed along the ray with a dynamic ray tracing. The computation is carried out with Babič's notation. In Appendix, Červený's notations are used. A similar derivation can be found in (Schleicher *et al.* 1993) for the isotropic case.

Using the chain rules, the second derivative of the traveltimes, wich define the matrix Ψ, can be rewritten in the ray coordinate system τ, α, β, with **P**, the slowness vector ($p_i = \frac{\partial\tau}{\partial x_i}$):

$$\frac{\partial^2\tau}{\partial x_i \partial x_k} = \frac{\partial p_i}{\partial\tau}\frac{\partial\tau}{\partial x_k} + \frac{\partial p_i}{\partial\alpha}\frac{\partial\alpha}{\partial x_k} + \frac{\partial p_i}{\partial\beta}\frac{\partial\beta}{\partial x_k}\; i, k = 1, 2, 3. \tag{15}$$

Because J is the Jacobian of the transformation from the general cartesian system to the ray coordinate system, the following relations exist, with $\nabla = (\frac{\partial}{\partial x_1}, \frac{\partial}{\partial x_2}, \frac{\partial}{\partial x_3})^T$, $[.\times.]$ the vectorial product and $(.,.)$ the scalar product:

$$\nabla\alpha = \frac{1}{J}\left[\frac{\partial\mathbf{x}}{\partial\beta}\times\mathbf{g}\right], \quad \nabla\beta = \frac{1}{J}\left[\mathbf{g}\times\frac{\partial\mathbf{x}}{\partial\alpha}\right],$$
$$\nabla\tau = \frac{1}{J}\left[\frac{\partial\mathbf{x}}{\partial\alpha}\times\frac{\partial\mathbf{x}}{\partial\beta}\right] = \mathbf{p}, \quad J = \left(\mathbf{g}, \left[\frac{\partial\mathbf{x}}{\partial\alpha}\times\frac{\partial\mathbf{x}}{\partial\beta}\right]\right). \tag{16}$$

Following (Kashtan & Petrashen 1983), the auxiliary orthogonal basis is introduced:

$$\mathbf{e}_1 = v\mathbf{p}; \quad \frac{d\mathbf{e}_k}{d\tau} = -\left(\mathbf{e}_k, \frac{\partial \mathbf{p}}{\partial \tau}\right)\mathbf{e}_1; \quad (k = 2, 3), \tag{17}$$

where v is the phase velocity.

The two-by-two transformation matrices **P**, **Q** and **T** are now defined. To be consistent with the auxiliary orthogonal basis, the elements of these matrices are numbered from 2 to 3, i.e.

$$\mathbf{Q} = \begin{pmatrix} \mathbf{Q}_{22} & \mathbf{Q}_{23} \\ \mathbf{Q}_{32} & \mathbf{Q}_{33} \end{pmatrix}$$

$$\begin{cases} \dfrac{\partial \mathbf{x}}{\partial \alpha} = \mathbf{Q}_{22}\mathbf{e}_2 + \mathbf{Q}_{32}\mathbf{e}_3; \\ \dfrac{\partial \mathbf{x}}{\partial \beta} = \mathbf{Q}_{23}\mathbf{e}_2 + \mathbf{Q}_{33}\mathbf{e}_3; \end{cases}$$

$$\begin{cases} \dfrac{\partial \mathbf{p}}{\partial \alpha} = \mathbf{P}_{22}\mathbf{e}_2 + \mathbf{P}_{32}\mathbf{e}_3 + \left(\dfrac{\partial \mathbf{p}}{\partial \alpha}, \mathbf{e}_1\right)\mathbf{e}_1; \\ \dfrac{\partial \mathbf{p}}{\partial \beta} = \mathbf{P}_{23}\mathbf{e}_2 + \mathbf{P}_{33}\mathbf{e}_3 + \left(\dfrac{\partial \mathbf{p}}{\partial \beta}, \mathbf{e}_1\right)\mathbf{e}_1; \end{cases} \tag{18}$$

$$\mathbf{T} = \mathbf{P}\mathbf{Q}^{-1}.$$

Replacing the first derivatives with their expressions defined in eqs (16) and (18), eq. (15) becomes:

$$\frac{\partial^2 \tau}{\partial x_i \partial x_k} = \frac{\partial p_i}{\partial \tau} p_k + \frac{\partial p_k}{\partial \tau} p_i - p_k p_i \left(\mathbf{g}, \frac{\partial \mathbf{p}}{\partial \tau}\right) + \mathbf{W}_{ik} \tag{19}$$

with

$$\mathbf{W} = \begin{pmatrix} (\mathbf{e}_2)_1 - (\mathbf{g}, \mathbf{e}_2)p_1 & (\mathbf{e}_3)_1 - (\mathbf{g}, \mathbf{e}_3)p_1 \\ (\mathbf{e}_2)_2 - (\mathbf{g}, \mathbf{e}_2)p_2 & (\mathbf{e}_3)_2 - (\mathbf{g}, \mathbf{e}_3)p_2 \end{pmatrix} \begin{pmatrix} \mathbf{T}_{22} & \mathbf{T}_{23} \\ \mathbf{T}_{32} & \mathbf{T}_{33} \end{pmatrix} \begin{pmatrix} (\mathbf{e}_2)_1 - (\mathbf{g}, \mathbf{e}_2)p_1 & (\mathbf{e}_2)_2 - (\mathbf{g}, \mathbf{e}_2)p_2 \\ (\mathbf{e}_3)_1 - (\mathbf{g}, \mathbf{e}_3)p_1 & (\mathbf{e}_3)_2 - (\mathbf{g}, \mathbf{e}_3)p_2 \end{pmatrix} \tag{20}$$

and

$$\det \mathbf{W} = \frac{g_3^2}{v^2} \det \mathbf{T}. \tag{21}$$

g is the group velocity vector and g_3 is its vertical component.

Applying the above calculation to the second derivatives of the reflected traveltime, $\tau^{(r)}$, and the diffracted traveltime, $\tau^{(d)}$, the matrix Ψ can be rewritten as follows:

$$\Psi = \begin{pmatrix} (\mathbf{e}_2)_1 - (\mathbf{g}, \mathbf{e}_2)p_1 & (\mathbf{e}_3)_1 - (\mathbf{g}, \mathbf{e}_3)p_1 \\ (\mathbf{e}_2)_2 - (\mathbf{g}, \mathbf{e}_2)p_2 & (\mathbf{e}_3)_2 - (\mathbf{g}, \mathbf{e}_3)p_2 \end{pmatrix} \begin{pmatrix} \mathbf{T}_{22}^{(r)} - \mathbf{T}_{22}^{(d)} & \mathbf{T}_{23}^{(r)} - \mathbf{T}_{23}^{(d)} \\ \mathbf{T}_{32}^{(r)} - \mathbf{T}_{32}^{(d)} & \mathbf{T}_{33}^{(r)} - \mathbf{T}_{33}^{(d)} \end{pmatrix} \begin{pmatrix} (\mathbf{e}_2)_1 - (\mathbf{g}, \mathbf{e}_2)p_1 & (\mathbf{e}_2)_2 - (\mathbf{g}, \mathbf{e}_2)p_2 \\ (\mathbf{e}_3)_1 - (\mathbf{g}, \mathbf{e}_3)p_1 & (\mathbf{e}_3)_2 - (\mathbf{g}, \mathbf{e}_3)p_2 \end{pmatrix}. \tag{22}$$

The determinant of Ψ is then equal to:

$$\det\Psi = \det\left(\mathbf{T}^{(r)} - \mathbf{T}^{(d)}\right)\left(\frac{g_3}{v}\right)^2. \tag{23}$$

The quantities of the incoming ray just before the reflection are denoted with the superscript (−) and the quantities of the outcoming ray just after the reflection are denoted with the superscript (+).

At the interface, the following relations exist (Kashtan *et al.* 1984):

$$\begin{cases} \dfrac{\partial \mathbf{x}^{(+)}}{\partial \alpha} = \dfrac{\partial \mathbf{x}^{(-)}}{\partial \alpha} + \dfrac{\mathbf{g}^{(+)} - \mathbf{g}^{(-)}}{(\mathbf{n}, \mathbf{g}^{(-)})}\left(\mathbf{n}, \dfrac{\partial \mathbf{x}^{(-)}}{\partial \alpha}\right) \\ \mathbf{p}^{(+)} = \mathbf{p}^{(-)} + h\mathbf{n}; \left(h = \frac{1}{(\mathbf{p}^{(+)} - \mathbf{p}^{(-)}, \mathbf{p}^{(+)} - \mathbf{p}^{(-)})^{\frac{1}{2}}}\right). \end{cases} \tag{24}$$

Using eqs (18) and (24) and assuming that e_2 is in the plane orthogonal to the incidence plane ($e_2^{(+)} = e_2^{(-)}$), the elements of the matrix $\mathbf{Q}^{(+)}$ can be expressed from the elements of the matrix $\mathbf{Q}^{(-)}$. Then the determinant of $\mathbf{Q}^{(+)}$ is equal to

$$\det\mathbf{Q}^{(+)} = \frac{v^{(-)}}{v^{(+)}} \frac{(\mathbf{n}, \mathbf{g}^{(+)})}{(\mathbf{n}, \mathbf{g}^{(-)})} \det\mathbf{Q}^{(-)}. \tag{25}$$

The ray from the source to the receiver can be split into two branches (see Fig. 1): a branch from the source to the reflection/scattered point, denoted branch 1, and a branch from the reflection/scattered point to the receiver, denoted branch 2. With the dynamic ray tracing along the branch 1, the quantities before the reflection point can be computed. The quantities after the reflection point need to be computed from the dynamic ray tracing along the branch 2.

Eq. (25) defines a relation between the initial values of the branch 2 and the final values of the branch 1. Remain to calculate $\det(\mathbf{T}^{(r)} - \mathbf{T}^{(d)})$ with the quantities of the branch 1 and branch 2.

To do so, following (Coddington & Levinson 1955), the fundamental matrix

$$\begin{pmatrix} \mathbf{Q}_1 & \mathbf{Q}_2 \\ \mathbf{P}_1 & \mathbf{P}_2 \end{pmatrix} \tag{26}$$

along the branch 2 is introduced. $\mathbf{P}_1$ and $\mathbf{Q}_1$ are the solutions of the dynamic ray tracing system with the initial conditions $\mathbf{P}_1 = 0$ and $\mathbf{Q}_1 = \mathbf{I}$. $\mathbf{P}_2$ and $\mathbf{Q}_2$ are the solutions of the dynamic ray tracing system with the initial conditions $\mathbf{P}_2 = \mathbf{I}$ and $\mathbf{Q}_2 = 0$. **I** is the two-by-two identity matrix.

The matrices **P** and **Q** along the branch 2 can then be expressed with the help of the fundamental matrix and the initial conditions $\mathbf{P}^{(+)}$ and $\mathbf{Q}^{(+)}$.

$$\begin{pmatrix} \mathbf{Q}(\tau) \\ \mathbf{P}(\tau) \end{pmatrix} = \begin{pmatrix} \mathbf{Q}_1 & \mathbf{Q}_2 \\ \mathbf{P}_1 & \mathbf{P}_2 \end{pmatrix} \begin{pmatrix} \mathbf{Q}^{(+)} \\ \mathbf{P}^{(+)} \end{pmatrix}. \tag{27}$$

Applying this relation for the 'diffracted' ray, where the initial point source condition is $\mathbf{Q}^{(d)(+)} = 0$, gives:

$$\mathbf{Q}^{(d)} = \mathbf{Q}_2\mathbf{P}^{(d)(+)}, \quad \mathbf{P}^{(d)} = \mathbf{P}_2\mathbf{P}^{(d)(+)};$$
$$\mathbf{T}^{(d)} = \mathbf{P}^{(d)}\mathbf{Q}^{(d)-1} = \mathbf{P}_2\mathbf{Q}_2^{-1}. \tag{28}$$

For the reflected ray, with the initial conditions $\mathbf{P}^{(r)(+)}$ and $\mathbf{Q}^{(r)(+)}$, and the symplectic properties of the fundamental matrix (Coddington & Levinson 1955), this gives:

$$\begin{aligned} \mathbf{P}^{(r)} &= -(\mathbf{Q}_2^{-1})^T\mathbf{Q}^{(r)(+)} + \mathbf{P}_2\mathbf{Q}_2^{-1}\mathbf{Q}^{(r)}; \\ \mathbf{T}^{(r)} &= \mathbf{P}^{(r)}\mathbf{Q}^{(r)-1} \\ &= -(\mathbf{Q}_2^{-1})^T\mathbf{Q}^{(r)(+)}\mathbf{Q}^{(r)-1}(\tau) + \mathbf{T}^{(d)}. \end{aligned} \tag{29}$$

The last equation gives a new expression for $\det(\mathbf{T}^{(r)} - \mathbf{T}^{(d)})$:

$$\det(\mathbf{T}^{(r)} - \mathbf{T}^{(d)}) = \frac{\det\mathbf{Q}^{(r)(+)}}{\det\mathbf{Q}_2 \det\mathbf{Q}^{(r)}} \tag{30}$$

Q_2 and $Q^{(r)}$ are evaluated at the receiver point. Because at the final point of the branch 2, $J = v \det \mathbf{Q}^{(r)}$, with J the Jacobian computed at the receiver position:

$$\det(\mathbf{T}^{(r)} - \mathbf{T}^{(d)}) = \frac{v}{J} \frac{\det \mathbf{Q}^{(r)(+)}}{\det \mathbf{Q}_2} \tag{31}$$

With eqs (23), (25) and (31), it is possible to rewrite $J \det(\Psi)$ as follows:

$$J \det \Psi = \frac{\det \mathbf{Q}^{(r)(-)}}{\det \mathbf{Q}_2} \frac{v^{(-)}}{v^{(+)}} \frac{(\mathbf{n}, \mathbf{g}^{(+)})}{(\mathbf{n}, \mathbf{g}^{(-)})} \frac{g_3^2}{v}. \tag{32}$$

The quantities g_3, v, are also evaluated at the receiver position.

The amplitude-preserving migration weights, eq. (14), are now rewritten with quantities computable along the rays by:

$$w(\hat{\mathbf{x}}_r) = \frac{\sqrt{\rho(\hat{\mathbf{x}}_r)}}{\varphi(\hat{\alpha}, \hat{\beta})(\mathbf{A}(\hat{\tau}, \hat{\alpha}, \hat{\beta}), \mathbf{d})} \sqrt{\frac{\det \mathbf{Q}^{(r)(-)}}{\det \mathbf{Q}_2^{(2)}} \frac{v^{(-)}}{v^{(+)}} \frac{g_3^2(\tau)}{v(\tau)}}. \tag{33}$$

The determinants of the matrices $\mathbf{Q}^{(r)(-)}$ and $\mathbf{Q}_2$ can be expressed with the Jacobians of the branch 1 (J_1) and the branch 2 (J_2):

$$J_1 = v^{(-)} \det \mathbf{Q}^{(r)(-)};$$
$$J_2 = v \det \mathbf{Q}^{(d)} = v \det \mathbf{Q}_2 \det \mathbf{P}^{(+)(d)} \tag{34}$$

With $\beta^{(+)}$ the longitudinal angle of the slowness vector $\mathbf{p}^{(+)}$ and eq. (18), the determinant of the matrix $\mathbf{P}^{(+)(d)}$ is equal to:

$$\det \mathbf{P}^{(d)(+)} = \frac{\sin \beta_+}{v^{(+)2}} \tag{35}$$

Therefore, substituting eq. (34) and eq. (35) into eq. (33) gives the following expression for the weight function:

$$w(\mathbf{x}_r) = \frac{\sqrt{\rho(\mathbf{x}_r)}}{\varphi(\alpha, \beta)(\mathbf{A}(\mathbf{x}_r), \mathbf{d})} g_3(\mathbf{x}_r) \frac{\sqrt{\sin \beta_+}}{v^{(+)}\sqrt{v^{(+)}}} \frac{\sqrt{J_1}}{\sqrt{J_2}}. \tag{36}$$

In order to implement eq. (36), the spreading for both branches of the ray need to be computed (Kashtan 1982). Other quantities in eq. (36) also can be computed during the ray tracing.

3 SMALL EXAMPLES

Before carrying out the sensitivity analysis, small examples are discussed. The first example is an 'inversion crime' because the same forward model is used to generate the data and to retrieve the reflectivity. The example is however used to study the effects of neglecting the anisotropy in the migration. In the second example, the data have been generated with a time-domain finite-difference code, therefore all the types of waves (converted, reflected, refracted) have been modelled. No uncorrelated or white noise have been added because the extraction of the reflectivity is done with a simple procedure. Indeed, the reflection coefficient is determined from the migrated image by picking the maximum amplitude at each trace and by dividing this amplitude by the maximum amplitude of the antiderivative of the source wavelet. It is recalled that the migration weights, eq. (14), do not contain the source term, therefore it is needed to remove the effect of the source to obtain the reflection coefficient from the migrated image.

Table 1. The parameters of layer and half space.

Media	ρ g cm^{-3}	V_{p0} km s^{-1}	V_{s0} km s^{-1}	ε	δ	γ
layer 1	2.0	1.8	0.9	0.2	0.15	0.2
half space	2.0	2.2	1.1	0.05	0.02	0.05

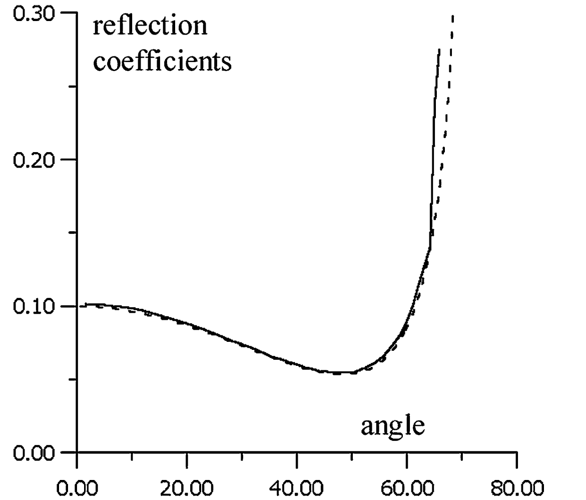

Figure 2. Example 1: the reflection coefficients: true (dashed line) and recovered (solid line).

3.1 Example 1

In the first example, the 3-D model is constituted by two vertical transverse isotropic (VTI) layers, separated by a flat interface. The distance between the source or receivers and the interface is 1 km. The second layer is a half space. The parameters of each layer are given in Table 1. V_{p0} and V_{s0} are the P and S vertical velocity, ρ is the density and ε, δ and γ are Thomsen's parameters (Thomsen 1986).

The synthetic data are generated using eq. (1). Only the vertical component is computed and only the P wave is considered. The geophones are regularly distributed in a horizontal box of 4 km by 4 km, with a 20 m spacing in each direction. The source wavelet is a Ricker wavelet. The 3D source pattern diagram φ is equal to $\sqrt{\sin \alpha}$, (α is the latitudinal take-off angle of the slowness vector at the source point).

The data are then migrated with the true parameters and the reflection coefficients are extracted. Fig. 2 shows the true and the retrieved reflection curve. Since the same forward model is used for the data generation and the migration, and the frequency of source wavelet is taken rather high [which makes stationary phase estimations eq. (9) exact], the two curves are identical (expect at the edge with the large angles). This is just a self consistent result. However, this approach is now used to show the effects of neglecting the anisotropy during the migration.

In Fig. 3, the reflectivity curves retrieved assuming an isotropic medium are plotted and compared with the correct one (curve 1). Notice, that for this example the anisotropy is weak, the relative difference between horizontal (V_{p1}) and vertical (V_{p0}) velocities is only about 17 per cent. The curve 3 of Fig. 3 corresponds to $V_{P0} = 1.8$ km s^{-1} and $\delta = \varepsilon = 0$. The error is large as expected, however in practice a different P-velocity would be used. Indeed, an optimal stack velocity would probably be found from a velocity analysis. For this case, a quick estimation of the optimal stack velocity, at least

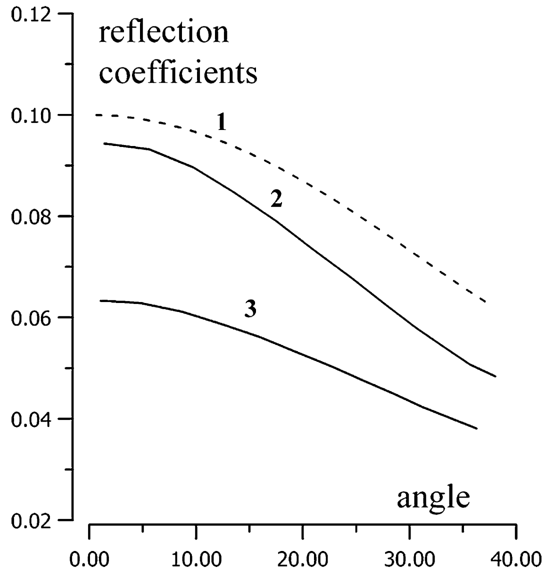

Figure 3. Example 1: True reflection coefficient (curve 1). The reflection coefficients, recovered in the case when the anisotropy of media is neglected: for $V_{P0} = 2.05$ km s^{-1} (curve 2) and for $V_{P0} = 1.8$ km s^{-1} (curve 3).

for the short offset, is about 2.05 km s^{-1}. The curve 2 corresponds to the reflection coefficient curve retrieved with an isotropic migration and $V_{P0} = 2.05$ km s^{-1}. In this case the error of the recovery of reflectivity is much smaller than in the previous case. However, the reflectivity values are smaller than the true ones for all offsets (the error is about 6 per cent for small angles and about 15–25 per cent for medium angles).

3.2 Example 2

It should be recalled that in the case of a pressure point source for high-frequency asymptotic, the pattern diagram is defined by the expression (Kashtan *et al.* 1984): for 3-D case:

$$\varphi(\hat{\alpha}, \hat{\beta}) = \frac{1}{4\pi \sqrt{\sin \hat{\alpha} \rho(\hat{\alpha}, \hat{\beta}) v(\hat{\alpha}, \hat{\beta})^{3/2}}}, \tag{37}$$

for 2-D case:

$$\varphi(\hat{\alpha}) = \frac{1}{4\pi \sqrt{\rho(\hat{\alpha})} v(\hat{\alpha})^{3/2}}. \tag{38}$$

During the processing of real data one should treat the definition of the pattern diagram carefully in the anisotropic case, because the phase velocity v depends on the direction of the slowness vector of the considered wave. This pattern diagram is used during the processing of the second example.

In the previous section, the data for the wavefield displacement were generated with the high-frequency formula. In this second example, the data, Fig. 4, are generated with a time-domain finite difference code. Therefore the data also contain converted and the refracted waves. The model is a 2-D model and the distance between the interface and the source or receivers is 0.5 km. The model parameters are given in Table 2.
The weight function for 2D case is:

$$w(\mathbf{x}_r) = \frac{\sqrt{\rho(\mathbf{x}_r)}}{\varphi(\alpha, \beta) A_3(\mathbf{x}_r)} g_3(\mathbf{x}_r) \frac{1}{v^{(+)}} \frac{\sqrt{J_1}}{\sqrt{J_2}}, \tag{39}$$

where J_1 and J_2 are calculated for the waves propagating in 2D media.

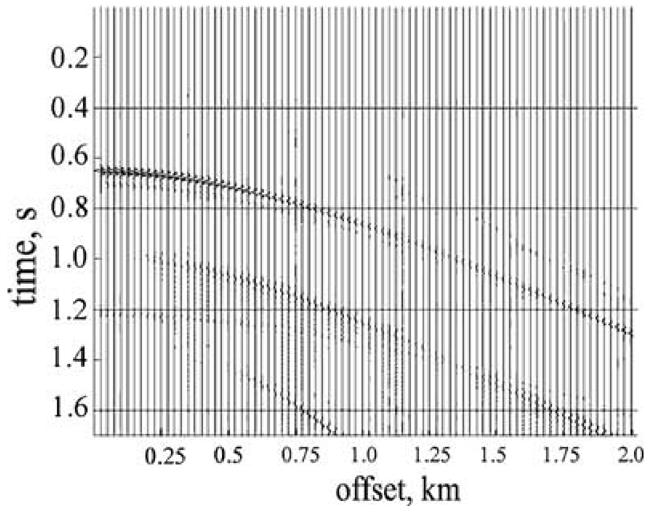

Figure 4. Example 2: the synthetic seismogram.

Table 2. The parameters of layer and half space.

Media	ρ g cm^{-3}	V_{p0} km s^{-1}	V_{s0} km s^{-1}	ε	δ	γ
layer 1	2.0	1.5	0.75	0.2	0.15	0.2
half space	2.0	1.8	1.05	0.05	0.02	0.05

The result of the amplitude-preserving migration is plotted Fig. 5. No tappers and filters have been implemented in the migration algorithm, because the goal of this study was only to test the anisotropy migration weights and to study the sensitivity of the reflectivity to the anisotropic parameters. In a production environment, wave decomposition and tappers would be applied to improve the migration image. The reflection coefficients are plotted Fig. 6. The retrieved reflection coefficient curve and the true one are similar showing the good quality of the weight function. The small discrepancies may be due to the finite frequency source wavelet taken for the forward modelling (for which the stationary phase estimation eq. (9) gives non-exact results). However the differences between the two curves in Fig. 5 are smaller than the ones observed in Fig 3.

4 SENSITIVITY ANALYSIS

Before processing real data, it is important to know the sensitivity of the amplitude-preserving migration formula to the anisotropic parameters, since it is not possible to retrieve all the parameters. The purpose is to find the most promising parametrization of the problem. Only the VTI case is considered in this paper. Notice that in this study, all the propagation effects are taken into account, notably the move out, the angle of incidence and the geometrical spreading.

When searching for the background (smooth/propagation) model parameters with VTI (layered) media, it has been shown (Alkalifah 1997) that the two main parameters that govern the propagation are the anisotropic NMO velocity $V_{\rm NMO}$ and η where

$$V_{\rm NMO} = V_{P0}\sqrt{1 + 2\delta} \text{ and } \eta = \frac{\varepsilon - \delta}{1 + 2\delta}. \tag{40}$$

When analysing the AVO/AVA responses, the most promising parametrization (Plessix & Bork 2000) is Z_{P0}, the vertical P-impedance, and $Z_{S0}(1 - \delta/2)$, the vertical S-impedance corrected by $1 - \delta/2$.

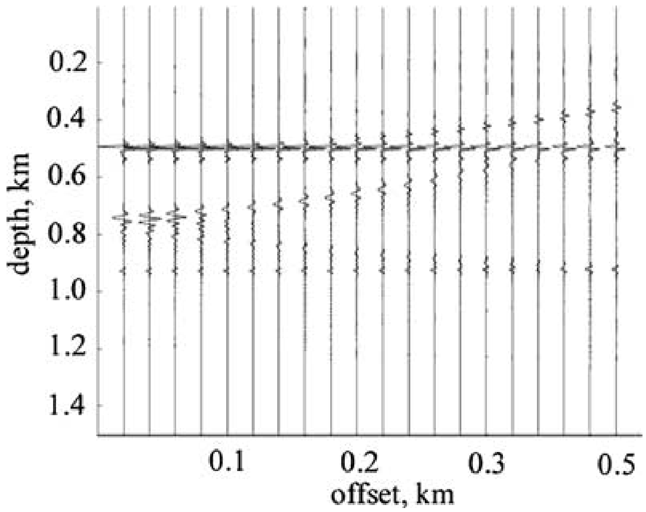

Figure 5. Example 2: the migrated section.

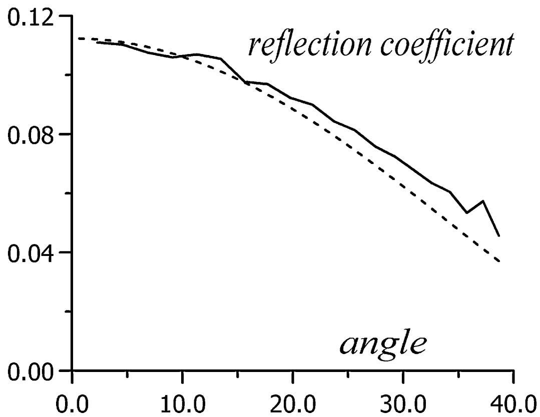

Figure 6. Example 2: true (dashed line) and recovered (solid line) reflection coefficients.

The amplitude-preserving migration formula aims to remove the effects of the geometrical spreading. It mainly depends on the background model parameters. It then seems natural to include in the parametrization $V_{\rm NMO}$ and η. Since in this paper, only the *P*-waves are considered, a possible parametrization, **b**, is V_{P0}, $V_{\rm NMO}$, η, ρ.

To obtain an indication of the sensitivity of each of the parameters, the following ratios, *R*, are defined:

$$R = \frac{b\partial\kappa}{\kappa\partial b} \text{ for } b = V_{p0}, V_{\rm NMO}, \rho;$$
$$R = \frac{\partial\kappa}{\kappa\partial b} \text{ for } b = \eta. \tag{41}$$

κ is the angle-dependent reflection coefficient. The ratio *R* is defined differently for the absolute quantities V_{P0}, $V_{\rm NMO}$, ρ, and for the relative quantity η.

Using the model described in Table 1, the different ratios, *R*, are plotted in Fig. 7 for a relative perturbation of 2.5 per cent of the model parameters. At small angles, the more sensitive parameter is $V_{\rm NMO}$ and at medium angles, the second more sensitive parameter is η. This result confirms the intuitive idea that these two background parameters are the most important ones in the anisotropic amplitude-preserving migration.

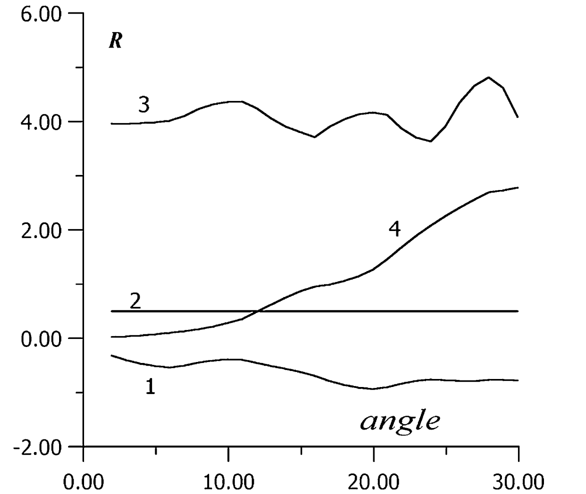

Figure 7. The ratio *R* versus angle for V_{p0} (curve 1), ρ (curve 2), $V_{\rm NMO}$ (curve 3), η (curve 4).

To complete this result and to find out what are the principal combinations of parameters that control the recovery of the reflection coefficient curve, a singular value decomposition (SVD) approach similar to that in (Plessix & Bork 2000) is used.

First an error function $S(\Delta\mathbf{b})$ is defined:

$$S(\Delta\mathbf{b}) = \sum_{i=1}^{n} \frac{[\kappa(\alpha_i, \Delta\mathbf{b}) - \kappa(\alpha_i, \Delta\mathbf{b}_0)]^2}{\kappa(\alpha_i, \Delta\mathbf{b}_0)^2}. \tag{42}$$

$\kappa(\alpha_i, \Delta\mathbf{b})$ is the reflection coefficient for the angle α_i $(i = 1, \ldots, n)$, retrieved with the perturbation, $\Delta\mathbf{b}$, of the model parameters. n is the number of observed data. $\kappa(\alpha_i, \Delta\mathbf{b}_0)$ is the reflection coefficient recovered with the true model parameters. The perturbation $\Delta\mathbf{b}$ is $\frac{\Delta V_{\rm NMO}}{V_{\rm NMO}}$, $\Delta\eta$, $\frac{\Delta V_{P0}}{V_{P0}}$, $\frac{\Delta\rho}{\rho}$.

The reflection coefficient $\kappa(\alpha_i, \Delta\mathbf{b})$ can be expanded into Taylor series near the value $\Delta\mathbf{b}_0 = (0, 0, 0, 0)$:

$$\kappa(\alpha_i, \Delta\mathbf{b}) = \kappa(\alpha_i, \Delta\mathbf{b}_0) + \sum_{j=1}^{4} \frac{\partial\kappa(\alpha_i, \Delta\mathbf{b}_0)}{\partial\Delta\mathbf{b}_j} \Delta\mathbf{b}_j. \tag{43}$$

The Jacobian rectangular matrix, **B**, is defined by

$$\mathbf{B}_{ij} = \frac{1}{\kappa(\alpha_i, \Delta\mathbf{b}_0)} \frac{\partial\kappa(\alpha_i, \Delta b)}{\partial\Delta b_j}, \tag{44}$$

where $1 \leq i \leq n$ and $1 \leq j \leq n_p$, with n_p the number of parameters. For small perturbations, using eq. (43), the error function, eq. (42), becomes:

$$S(\Delta\mathbf{b}) = \Delta\mathbf{b}^T \mathbf{H} \Delta\mathbf{b}; \tag{45}$$

with $\mathbf{H} = \mathbf{B}^T\ \mathbf{B}$ a n_p by n_p matrix.

Notice that the matrix **B** can be numerically obtained from the retrieved reflection coefficients by finite differences.

The singular value decomposition of **H** gives:

$$\mathbf{H} = \mathbf{D}^T \Lambda \mathbf{D}, \tag{46}$$

with $(1 \leq j \leq n_p, 1 \leq k \leq n_p)$

$$\Lambda_{jk} = \lambda_j \delta_{jk}; \quad \mathbf{D}_{jk} = \mathbf{E}_k^{(j)}. \tag{47}$$

λ_j is the *j*-th eigenvalue of **H** and $\mathbf{E}^{(j)}$ is the associated eigenvector.

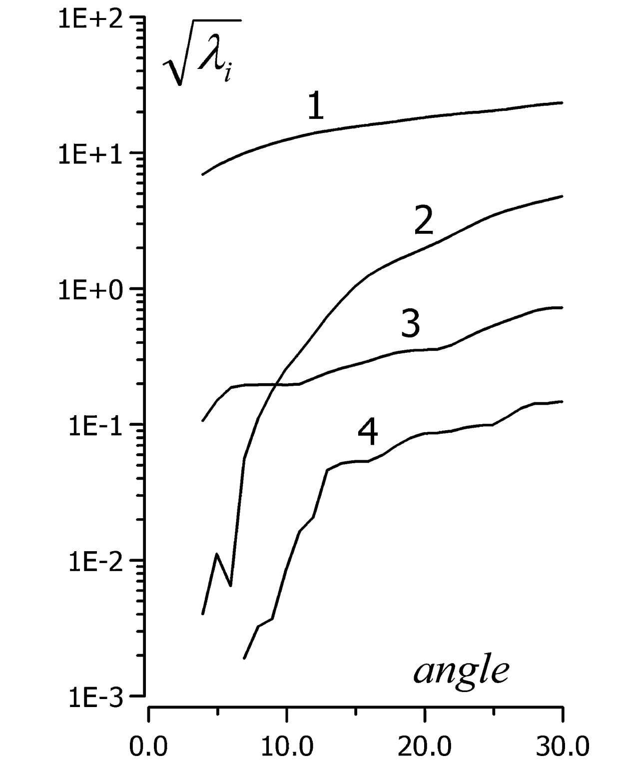

Figure 8. The eigenvalues of the correlation matrix versus the maximal angle α_n. The number near each curve corresponds to the number of the eigenvalue.

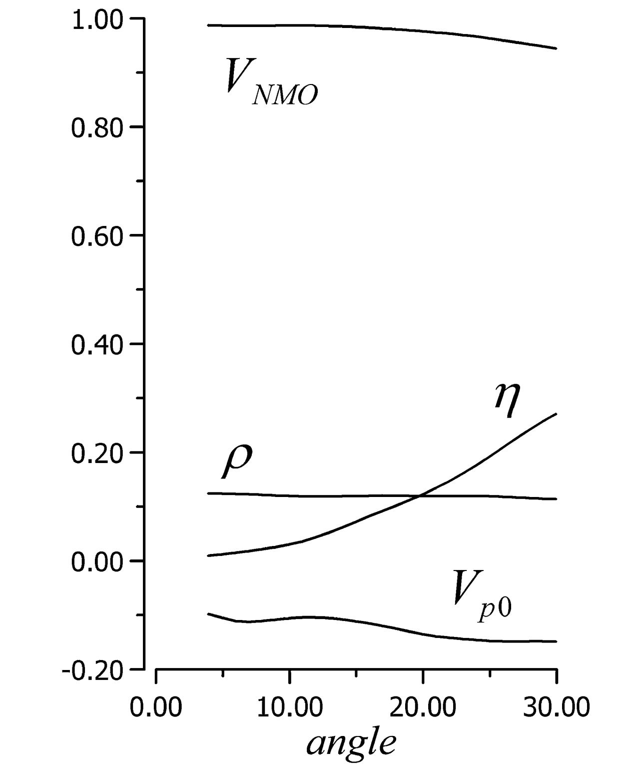

Figure 9. The components of the first eigenvector versus the maximal angle α_n.

The error function can be rewritten as follows:

$$S(\Delta \mathbf{b}) = \sum_{j=1}^{n_p} \lambda_j (\Delta \mathbf{b}, \mathbf{E}^{(j)})^2$$
$$= || \sum_{j=1}^{n_p} \sqrt{\lambda_j} (\Delta \mathbf{b}, \mathbf{E}^{(j)}) \mathbf{E}^{(j)} ||^2. \qquad (48)$$

The error in the reflection coefficients retrieved with non-correct parameters is a weighted sum of the parametrization $(\Delta \mathbf{b}, \mathbf{E}^{(j)})$. The weight of the j−th combination is $\sqrt{\lambda_j}$.

The eigenvalues (see Fig. 8) are sorted from the largest one to the smallest one. Numerically, the ratio $\frac{\sqrt{\lambda_1}}{\sqrt{\lambda_3}}$ is almost always larger than 30 when the maximum angle α is smaller than 30 degrees. This means that only two (combinations of) parameters play a significant role. In fact, for small angles, smaller than 10 degrees, the ratio $\frac{\sqrt{\lambda_1}}{\sqrt{\lambda_2}}$ is also larger than 30. This ratio decreases up to 5 for a maximum angle of 30 degrees. Therefore, the second combination of parameters plays a role only at medium angles.

The two main (combinations of) parameters are given by the first and the second eigenvectors. The components of the first and second eigenvectors are plotted in Figs 9 and 10. The first eigenvector is almost in the direction of V_{NMO} and the second eigenvector is in the direction of η. These results show that V_{NMO} and η are the two main parameters needed to perform a VTI amplitude-preserving migration. Similar results have been obtained with different models. For this case, the ratio $\frac{\sqrt{\lambda_1}}{\sqrt{\lambda_2}}$ is around 5 at medium angles. Neglecting the second parameter then creates an error of about 20 per cent in the amplitudes at medium angles. This more or less corresponds to the isotropic case, when the only parameter used to migrate the data is an optimal stack velocity and this corroborates the result found in example 1.

In Appendix B, the same analysis is performed with a different parametrization. The results with this different parametrization leads to the same conclusions.

5 CONCLUSIONS AND DISCUSSIONS

An amplitude-preserving migration algorithm for anisotropic media has been proposed. The migration is based on a weighted diffraction stack. The migration weights are calculated after Fourier transform of the stacking integral with the stationary phase theorem. They are valid for the high-frequency regime. The weights are formulated with quantities computable during the ray tracing in order to obtain a formula relatively easy to implement. Some simple synthetic examples have shown the correctness of these migration weights and the importance of taking into account the anisotropy in the amplitude-preserving migration algorithm when using medium angles.

For vertical transverse isotropic media, a sensitivity analysis has showed that two main parameters are needed, the anisotropic NMO velocity, V_{NMO}, and the parameter η when only the P-waves are considered. These parameters can be recovered by NMO analysis or traveltime inversion as shown in (Alkalifah & Rampton 2001). This interesting result means that an amplitude-preserving migration and AVO/AVA analysis can be carried out after a model building (velocity) analysis in the vertical transverse isotropic case.

ACKNOWLEDGMENTS

The authors would like to thank Peter Bakker for his advice and the review of this work. The computations were performed on the high-performance cluster of Peterhof Communication Center of Saint-Petersburg State University. This work was supported by the CRDF

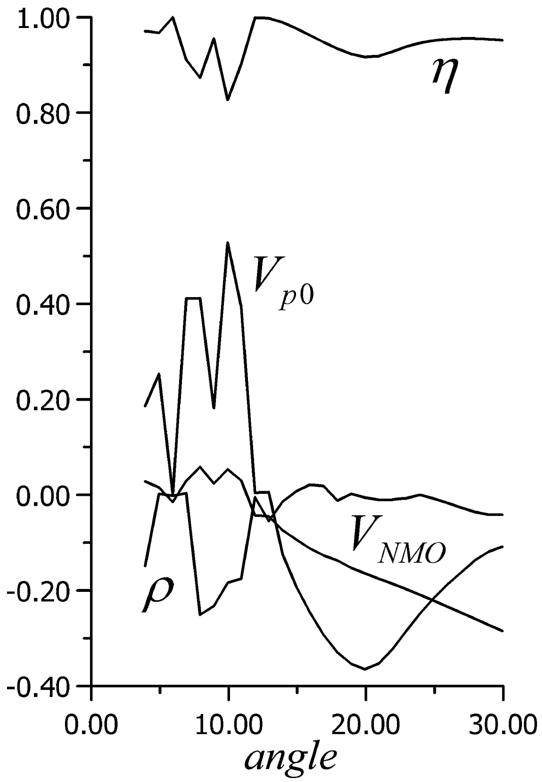

Figure 10. The components of the second eigenvector versus the maximal angle α_n.

grant RG0-1318(3)-ST-02, the grant RFBR 03-05-06153 and the grant A03-2.13-366. The authors would also like to thank the two reviewers, Professors Jean Virieux and Kees Wapenaar, for their comments.

REFERENCES

Alkhalifah, T., 1997. Velocity analysis using nonhyperbolic moveout in transversely isotropic media, *Geophysics,* **62,** 1839–1854.

Alkhalifah, T. & Rampton, D., 2001. Seismic anisotropy in Trinidad: A new tool for lithology prediction, *The Leading Edge,* **20**, 4, 420–424.

Babič, V. M., 1961. Ray method of calculating the intensity of wavefronts in the case of a heterogeneous, anisotropic, elastic medium, *Problems of the Dynamic Theory of Propagation of Seismic Waves,* **5,** 36 [English transl.: *Geophys. J. Int.,* **118** 379, 1994].

Bakker, P. M., 1996. Theory of anisotropic dynamic ray tracing in ray-centred coordinates, *Pageoph,* **148,** 583–589.

Beylkin, G., 1985. Imaging of discontinuities in the inverse scattering problem by inversion of a causal generalized Randon transform, *J. math. Phys.,* **26**, 99–108.

Beylkin, G. & Burridge, R., 1990. Linearized inverse scattering problems in acoustics and elasticity, *Wave motion,* **12,** 15–52.

Bleistein, N., 1987. On the imaging of the reflectors in the earth, *Geophysics,* **52,** 931–942.

Bortfeld, R., 1989. Geometrical ray theory: Rays and traveltimes in seismic systems (second-order approximations of the traveltimes), *Geophysics,* **54,** 342–349.

Cerveny, V., 2001. *Seismic ray theory*, Cambridge University Press, p. 713

Chavent, G. & Plessix, R.-E., 1999. An optimal true amplitude least-squares prestack depth migration, *Geophysics,* **64,** 508–515.

Coddington, E.A. & Levinson, N., 1955. *Theory of ordinary differential equations*, New York, Toronto, London.

Docherty, P., 1991. A brief comparison of some Kirchhoff integral formula for migration and inversion, *Geophysics,* **56,** 1164–1169.

Goldin, S.V., 1989. Method of discontinuities and theoretical problems of migration, 59th Ann. Int. Mtg., SEG, Expanded Abstract, 1326–1328.

Hanitzsch, C., 1997. Comparison of weights in prestack amplitude-preserving Kirchhoff depth migration, *Geophysics,* **62,** 1812–1816.

Jin, S., Madariaga, R., Virieux, J. & Lambaré, G., 1992. Two-dimensional asymptotic iterative elastic inversion, *Geophys. J. Int.,* **108,** 575–588.

Kashtan, B. M., 1982. On calculation of geometrical spreading in piecewisely homogeneous anisotropic elastic media, *Problems of the Dynamic Theory of Propagation of Seismic Waves,* **22,** 14.

Kashtan, B.M. & Petrashen, G.I., 1983. On calculation of geometrical spreading in inhomogeneous anisotropic elastic media, *Problems of the Dynamic Theory of Propagation of Seismic Waves,* **23,** 31.

Kashtan, B.M., Kovtun, A.A. & Petrashen, G.I., 1984. Algorithms of calculation of body wavefields in arbitrary anisotropic elastic medium, *Propagation of body waves and methods of calculation of wave fields in anisotropic elastic medium*, Leningrad.

Keho, T.H. & Beydoun, B., 1988. Paraxial ray Kirchhoff migration, *Geophysics,* **53**, 12,1540–1546.

Lailly, P., 1983. The seismic inverse problem as a sequence of before stack migration, *In Proc. of Conf. on Inverse Scattering, Theory and Applications, Philadelphia, SIAM*.

Lambaré, G., Virieux, J., Madariaga, R. & Jin, S., 1992. Iterative asymptotic inversion in the acoustic approximation, *Geophysics,* **57,** 1138–1154.

Lambaré, G., Operto, S., Podvin, P. & Thierry, P., 2003. 3D ray-Born migration/inversion—Part 1: theory, *Geophysics,* **68,** 1348–1356.

Miller, D., Oristaglio, M. & Beyklin, G., 1987. A new slant on seismic imaging—Migration and integral geometry, *Geophysics,* **52,** 943–964.

Plessix, R.-E. & Bork, J., 1998. A full waveform inversion example in VTI media, *68th Ann. Internat. Mtg: Soc. of Expl. Geophys.,* 1562–1565.

Plessix, R.-E. & Bork, J., 2000. Quantitative estimate of VTI parameters from AVA responses, *Geophys. Prospec.,* **48,** 87.

Schleicher, J., Filpo, E., Hanitzsch, C. Hubral, P. & Tygel, M., 1993. Amplitude-preserving migration using diffraction stacks, *38th. Ann. Int. Mtg., SPIE, Proceedings, Mathematical Methods in Geophysical Imaging,* **2003**, 97–108.

Tarantola, A., 1984. Inversion of seismic reflection data in the acoustic approximation, *Geophysics,* **49**, (8), 1259–1266.

ten Kroode, A.P.E., Smit, D.J. & Verdel, A.R., 1994. Linearized inverse scattering in the presence of caustics, *SPIE annual meeting, San Diego*, Exp. Abstract.

Thierry, P., Operto, S. & Lambaré, G., 1999. Fast 2D ray+Born migration/inversion in complex media, *Geophysics,* **34,** 162–182.

Thomsen, L., 1986. Weak elastic anisotropy, *Geophysics,* **51,** 1954–1966.

APPENDIX A: WEIGHT FUNCTION WITH ČERVENÝ'S NOTATIONS

In this section, Červený's notation (Červený 2001) are used to rewrite the weight function, eq. (33). The ray coordinate system is (γ_1, γ_2, T) (Červený 2001 3.10.2).

A1 detΨ

With $\mathbf{p} = \nabla T$, the slowness vector, and using the chain rules, the second derivatives of the traveltimes can be rewritten as follows:

$$\frac{\partial^2 T}{\partial x_i \partial x_k} = \frac{\partial p_i}{\partial T}\frac{\partial T}{\partial x_k} + \frac{\partial p_i}{\partial \gamma_1}\frac{\partial \gamma_1}{\partial x_k} + \frac{\partial p_i}{\partial \gamma_2}\frac{\partial \gamma_2}{\partial x_k}. \tag{49}$$

J is now the Jacobian of the transformation from the general cartesian coordinate system to the ray coordinate system, therefore:

$$\nabla\gamma_1 = \frac{1}{J}\left[\frac{\partial \mathbf{x}}{\partial\gamma_1}\times\mathbf{U}\right],\quad \nabla\gamma_2 = \frac{1}{J}\left[\mathbf{U}\times\frac{\partial \mathbf{x}}{\partial\gamma_2}\right],$$
$$\nabla\tau = \frac{1}{J}\left[\frac{\partial \mathbf{x}}{\partial\gamma_1}\times\frac{\partial \mathbf{x}}{\partial\gamma_2}\right] = \mathbf{p},\quad J = \left(\mathbf{g},\left[\frac{\partial \mathbf{x}}{\partial\gamma_1}\times\frac{\partial \mathbf{x}}{\partial\gamma_2}\right]\right). \tag{50}$$

with $\mathbf{U}$ the group velocity vector (Červený 2001 2.2.65), $[.\times.]$ the vector product, and $(.,.)$ the scalar product.

The ray-centred basis vectors are defined by (Červený 2001, 4.2.17, Bakker 1996, 5a), with $I = 1, 2$:

$$\mathbf{e}_3 = v\mathbf{p} = C\mathbf{p};\quad \frac{d\mathbf{e}_I}{dT} = -(\mathbf{e}_I, \frac{\partial\mathbf{p}}{\partial T})\mathbf{e}_3; \tag{51}$$

with $C = v$ the phase velocity.

The transformation matrices $\mathbf{Q}_{IJ} = \frac{\partial x_I}{\partial\gamma_J}$, and $\mathbf{P}_{IJ} = \frac{\partial p_I}{\partial\gamma_J}$ (Červený 2001, 4.2.35, Bakker 1996, 6) and $\mathbf{M}_{IJ}$ (Červený 2001 4.2.37), with $I, J = 1, 2$, are now formed:

$$\frac{\partial\mathbf{x}}{\partial\gamma_1} = \mathbf{Q}_{11}\mathbf{e}_1 + \mathbf{Q}_{21}\mathbf{e}_2;$$
$$\frac{\partial\mathbf{x}}{\partial\gamma_2} = \mathbf{Q}_{12}\mathbf{e}_1 + \mathbf{Q}_{22}\mathbf{e}_2;$$
$$\frac{\partial\mathbf{p}}{\partial\gamma_1} = \mathbf{P}_{11}\mathbf{e}_1 + \mathbf{P}_{21}\mathbf{e}_2 + \left(\frac{\partial\mathbf{p}}{\partial\gamma_1},\mathbf{e}_3\right)\mathbf{e}_3;$$
$$\frac{\partial\mathbf{p}}{\partial\gamma_2} = \mathbf{P}_{12}\mathbf{e}_1 + \mathbf{P}_{22}\mathbf{e}_2 + \left(\frac{\partial\mathbf{p}}{\partial\gamma_2},\mathbf{e}_3\right)\mathbf{e}_3;$$
$$\mathbf{M}_{IJ} = \mathbf{P}\mathbf{Q}^{-1}. \tag{52}$$

With these definitions of the ray-centred basis and the transformation matrices, eq. (49), becomes after some calculations:

$$\frac{\partial^2 T}{\partial x_i\partial x_k} = \frac{\partial p_i}{\partial T}p_k + \frac{\partial p_k}{\partial T}p_i - p_k p_i\left(\mathbf{U},\frac{\partial\mathbf{p}}{\partial T}\right) + \mathbf{W}_{ik} \tag{53}$$

with

$$\mathbf{W} = \begin{pmatrix}(\mathbf{e}_1)_1 - (\mathbf{U},\mathbf{e}_1)p_1 & (\mathbf{e}_2)_1 - (\mathbf{U},\mathbf{e}_2)p_1\\ (\mathbf{e}_1)_2 - (\mathbf{U},\mathbf{e}_1)p_2 & (\mathbf{e}_2)_2 - (\mathbf{U},\mathbf{e}_2)p_2\end{pmatrix}$$
$$\begin{pmatrix}\mathbf{M}_{11} & \mathbf{M}_{12}\\ \mathbf{M}_{21} & \mathbf{M}_{22}\end{pmatrix}$$
$$\begin{pmatrix}(\mathbf{e}_1)_1 - (\mathbf{U},\mathbf{e}_1)p_1 & (\mathbf{e}_1)_2 - (\mathbf{U},\mathbf{e}_1)p_2\\ (\mathbf{e}_2)_1 - (\mathbf{U},\mathbf{e}_2)p_1 & (\mathbf{e}_2)_2 - (\mathbf{U},\mathbf{e}_2)p_2\end{pmatrix}. \tag{54}$$

Formulae (53) and (54) can be applied to the diffracted and reflected traveltimes. Using the superscript, (r), for the reflected ray and the superscript, (d), for the diffracted ray, the matrix Ψ becomes:

$$\Psi = \begin{pmatrix}(\mathbf{e}_1)_1 - (\mathbf{U},\mathbf{e}_1)p_1 & (\mathbf{e}_2)_1 - (\mathbf{U},\mathbf{e}_2)p_1\\ (\mathbf{e}_1)_2 - (\mathbf{U},\mathbf{e}_1)p_2 & (\mathbf{e}_2)_2 - (\mathbf{U},\mathbf{e}_2)p_2\end{pmatrix}$$
$$\begin{pmatrix}\mathbf{M}^{(r)}_{11} - \mathbf{M}^{(d)}_{11} & \mathbf{M}^{(r)}_{12} - \mathbf{M}^{(d)}_{12}\\ \mathbf{M}^{(r)}_{21} - \mathbf{M}^{(d)}_{21} & \mathbf{M}^{(r)}_{22} - \mathbf{M}^{(d)}_{22}\end{pmatrix}$$
$$\begin{pmatrix}(\mathbf{e}_1)_1 - (\mathbf{U},\mathbf{e}_1)p_1 & (\mathbf{e}_1)_2 - (\mathbf{U},\mathbf{e}_1)p_2\\ (\mathbf{e}_2)_1 - (\mathbf{U},\mathbf{e}_2)p_1 & (\mathbf{e}_2)_2 - (\mathbf{U},\mathbf{e}_2)p_2\end{pmatrix}. \tag{55}$$

And the determinant is equal to:

$$\det\Psi = \frac{U_3^2}{C^2}\det(\mathbf{M}^{(r)} - \mathbf{M}^{(d)}). \tag{56}$$

U_3 is the vertical component of $\mathbf{U}$.

A2 Relation at the interface

The ray from the source to the receiver can be split into two branches: one from the source to the scattered point (for the diffracted ray) or to the reflection point (for the reflection ray), called branch 1, and one from the scattered or reflection point to the receiver point, called branch 2. The quantities of the branch 1 just before the scattered or reflection point are denoted with the superscript $(-)$, and the quantities of the branch 2 just after this point are denoted with the superscript $(+)$.

The interface is not known when the migration is performed. A 'virtual' interface is then locally defined at the scattered point by its normal, $\mathbf{n}$, which is given by

$$\mathbf{n} = \frac{\mathbf{p}^{(+)} - \mathbf{p}^{(-)}}{(\mathbf{p}^{(+)} - \mathbf{p}^{(-)}, \mathbf{p}^{(+)} - \mathbf{p}^{(-)})^{\frac{1}{2}}}. \tag{57}$$

The relation between the two branches is:

$$\frac{\partial x^{(+)}}{\partial\gamma_1} = \frac{\partial x^{(-)}}{\partial\gamma_1} + \frac{\mathbf{U}^{(+)} - \mathbf{U}^{(-)}}{(\mathbf{n},\mathbf{U}^{(-)})}\left(\mathbf{n},\frac{\partial x^{(-)}}{\partial\gamma_1}\right). \tag{58}$$

With $e_2^{(+)} = e_2^{(-)}$ and e_2 in the plane orthogonal to the incident plane, the matrix $\mathbf{Q}^{(+)}$ can be expressed with the matrix $\mathbf{Q}^{(-)}$ by

$$\mathbf{Q}^{(+)}_{21} = a\mathbf{Q}^{(-)}_{21},\quad \mathbf{Q}^{(+)}_{11} = \mathbf{Q}^{(-)}_{11} + b\mathbf{Q}^{(-)}_{21}$$
$$\mathbf{Q}^{(+)}_{22} = a\mathbf{Q}^{(-)}_{22},\quad \mathbf{Q}^{(+)}_{12} = \mathbf{Q}^{(-)}_{12} + b\mathbf{Q}^{(-)}_{22} \tag{59}$$

with

$$a = \frac{C^{(-)}}{C^{(+)}}\frac{(\mathbf{n},\mathbf{U}^{(+)})}{(\mathbf{n},\mathbf{U}^{(-)})}\text{ and } b = (e_2^{(+)}, \mathbf{U}^{(+)} - \mathbf{U}^{(-)})\frac{(\mathbf{n},\mathbf{U}^{(+)})}{(\mathbf{n},\mathbf{U}^{(-)})}$$

Therefore

$$\det\mathbf{Q}^{(+)} = \frac{C^{(-)}}{C^{(+)}}\frac{(\mathbf{n},\mathbf{U}^{(+)})}{(\mathbf{n},\mathbf{U}^{(-)})}\det\mathbf{Q}^{(-)}. \tag{60}$$

A3 det($\mathbf{M}^{(r)} - \mathbf{M}^{(d)}$)

In the previous subsection, the final values, $\mathbf{Q}^{(-)}$, of the branch 1, have been related to the initial values, $\mathbf{Q}^{(+)}$, of the branch 2. The next step is then to rewrite $\det(M^{(r)} - M^{(d)})$ with the initial and final conditions of $\mathbf{Q}$ on the branch 2.

Following Červený (Červený 2001,Section 4.3.1), $\mathbf{P}_1$ and $\mathbf{Q}_1$ are the solutions of the dynamic ray tracing along the branch 2 with the initial conditions $\mathbf{P}_1 = 0$ and $\mathbf{Q}_1 = \mathbf{I}$ ($\mathbf{I}$ is the two-by-two identity matrix). $\mathbf{P}_2$ and $\mathbf{Q}_2$ are the solutions of the dynamic ray tracing with the initial conditions $\mathbf{P}_2 = \mathbf{I}$ and $\mathbf{Q}_2 = 0$. The propagator matrix (Červený 2001, 4.3.5) is

$$\begin{pmatrix}\mathbf{Q}_1^{(2)} & \mathbf{Q}_2^{(2)}\\ \mathbf{P}_1^{(2)} & \mathbf{P}_2^{(2)}\end{pmatrix}. \tag{61}$$

With the initial conditions $\mathbf{P}^{(+)}$ and $\mathbf{Q}^{(+)}$, at any point on the branch 2 the matrices $\mathbf{P}$ and $\mathbf{Q}$ verify (Červený 2001, 4.14.15):

$$\begin{pmatrix}\mathbf{Q}\\ \mathbf{P}\end{pmatrix} = \begin{pmatrix}\mathbf{Q}_1 & \mathbf{Q}_2\\ \mathbf{P}_1 & \mathbf{P}_2\end{pmatrix}\begin{pmatrix}\mathbf{Q}^{(+)}\\ \mathbf{P}^{(+)}\end{pmatrix}, \tag{62}$$

For the 'diffracted' ray, $\mathbf{Q}^{(d)(+)} = 0$, this gives:

$$\mathbf{Q}^{(d)} = \mathbf{Q}_2\mathbf{P}^{(d)(+)},\ \mathbf{P}^{(d)} = \mathbf{P}_2\mathbf{P}^{(d)(+)}$$
$$\mathbf{M}^{(d)} = \mathbf{P}\mathbf{Q}^{-1} = \mathbf{P}_2\mathbf{Q}_2^{-1}. \tag{63}$$

For the reflected ray, using the symplectic properties of the propagator matrix (Červený 2001, 4.3.16), this gives:

$$\mathbf{P}^{(r)} = -\left(\mathbf{Q}_2^{-1}\right)^T\mathbf{Q}^{(r)(+)} + \mathbf{P}_2\mathbf{Q}_2^{-1}\mathbf{Q}^{(r)};$$
$$\mathbf{M}^{(r)} = -\left(\mathbf{Q}_2^{-1}\right)^T\mathbf{Q}^{(r)(+)}\mathbf{Q}^{(r)-1} + \mathbf{M}^{(d)}. \tag{64}$$

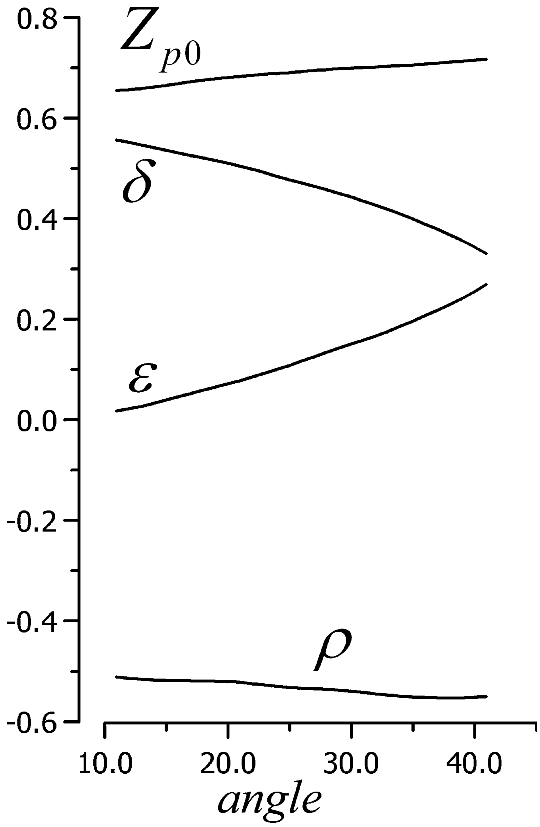

Figure 11. The components of the first eigenvector versus the maximal angle α_n.

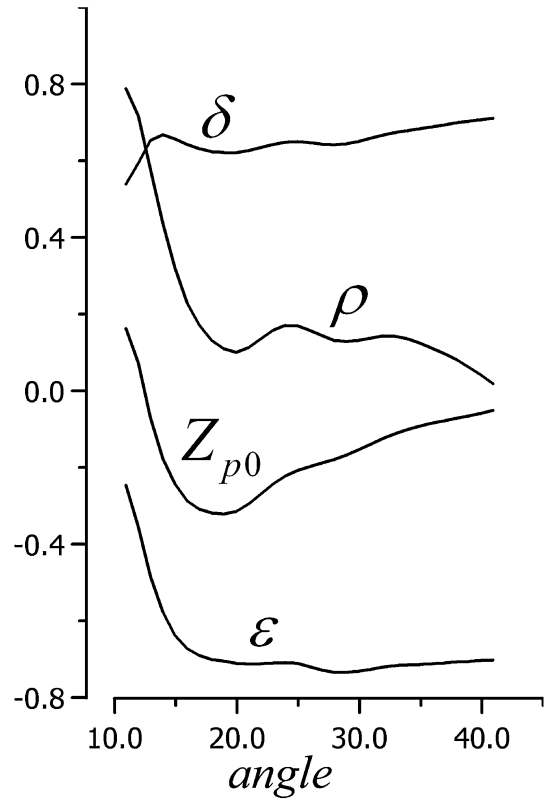

Figure 12. The components of the second eigenvector versus the maximal angle α_n.

In this way

$$\det(\mathbf{M}^{(r)} - \mathbf{M}^{(d)}) = \frac{\det\mathbf{Q}^{(r)(+)}}{\det\mathbf{Q}_2 \det Q^{(r)}}. \quad (65)$$

A4 New expression for the weight function

With (Červený 2001, 4.2.97)

$J = C\det\mathbf{Q}^{(r)}$

and the formulae (60) and (65), $\det\Psi$, eq. (56), is equal to

$$\det\Psi = \frac{\det\mathbf{Q}^{(r)(-)}}{J\det\mathbf{Q}_2^{(2)}} \frac{C^{(-)}}{C^{(+)}} \frac{(\mathbf{n}, \mathbf{U}^{(+)})}{(\mathbf{n}, \mathbf{U}^{(-)})} \frac{U_3^2}{C}. \quad (66)$$

Replacing $\det\Psi$ in eq. (33) by its expression, eq. (66), gives the new expression for the amplitude-preserving weight function:

$$w(\hat{\mathbf{x}}_r) = \frac{\sqrt{\rho(\hat{\mathbf{x}}_r)}}{\varphi(\hat{\gamma}_1, \hat{\gamma}_2)(\mathbf{A}(\hat{T}, \hat{\gamma}_1, \hat{\gamma}_2), \mathbf{d})} \sqrt{\frac{\det\mathbf{Q}^{(r)(-)}}{\det\mathbf{Q}_2^{(2)}} \frac{C^{(-)}}{C^{(+)}} \frac{U_3^2}{C}} \quad (67)$$

APPENDIX B: SENSITIVITY ANALYSIS WITH ANOTHER PARAMETRIZATION

In this appendix, the parametrization of the problem for the acoustic case is (Z_{P0}, ρ, ε, δ). Using the approach explained previously, a singular value decomposition is performed to find the combinations of parameters which have the large impact on the result. The ratios of the eigenvalues show that only two combinations of parameters can be effectively retrieved with noisy data. The perturbation, $\Delta\mathbf{b}$, is now ($\frac{\Delta Z_{P0}}{Z_{P0}}$, $\frac{\Delta\rho}{\rho}$, $\Delta\varepsilon$, $\Delta\delta$). The first eigenvector, Fig. 11, mainly depends on $\frac{\Delta Z_{P0}}{Z_{P0}}$, $-\frac{\Delta\rho}{\rho}$ and $\Delta\delta$. The second eigenvector, Fig. 12, mainly depends on $\Delta\delta$ and $-\Delta\varepsilon$. If C_1 and C_2 are the two main (combinations of) parameters which govern the recovery of the reflection curve in the amplitude-preserving migration, the results indicate that C_1 and C_2 should more or less verify:

$$\left|\frac{\Delta C_1}{C_1}\right| = \left|\frac{\Delta Z_{P0}}{Z_{P0}} + \Delta\delta - \frac{\Delta\rho}{\rho}\right|$$
$$|\Delta C_2| = |\Delta\delta - \Delta\varepsilon|. \quad (68)$$

$V_{\mathrm{NMO}} = V_{P0}\sqrt{1+2\delta} = \frac{Z_{P0}}{\rho}\sqrt{1+2\delta}$ and $\eta = \frac{\varepsilon-\delta}{1+2\delta}$ verify the conditions on C_1 and C_2 at least for small values of ε and δ. Then V_{NMO} and η are the two main parameters.